Available online at www.sciencedirect.com

ScienceDirect

Transportation Research Procedia 45 (2020) 384–393

Transportation Research Procedia

www.elsevier.com/locate/procedia

AIIT 2nd International Congress on Transport Infrastructure and Systems in a changing world (TIS ROMA 2019), 23rd-24th September 2019, Rome, Italy

A risk assessment method for "Eurobalise" fastening system: managing the sensor/sleeper interaction in the high-speed railway infrastructure

Andrea Simone[a,*], Claudio Lantieri[a], Valeria Vignali[a], Francesco Mazzotta[a], Michele Carpinone[a], Federico Cuppi[a,b], Marco Nanni[b], Davide Davalli[b]

[a]*DICAM Department, School of Engineering and Architecture, University of Bologna, Viale Risorgimento 2, 40136, Bologna , Italy*
[b]*Alstom Ferroviaria, Via di Corticella 75, 40128, Bologna , Italy*

Abstract

The aim of this research is to define a breakage limit for the fastening system of the "Eurobalise" device of the ERTMS/ETCS rail signalling system on the European railways. The widespread presence of the system along the European railway line and the increasing of high-speed lines have led the research to find design solutions able to increase the attack system strength, avoiding its detachment from the sleepers. Mechanical tests on tensile, shear and bending configurations have been carried out to evaluate the jointing systems between Eurobalise and sleepers. Additional full-scale tests allowed the definition of the load actions and of the breaking points. The connection between balise and sleepers is able to react to the train's aerodynamic actions, confirming the system reliability even for the passage of high-speed trains. Through the experimental approach were defined standard test procedures useful to improve the sheet data of this kind of fastening system.

Keywords: Eurobalise; ERTMS; train; high-speed railway; slipstream

1. Introduction

The need to ensure trains interoperability between European nations led the European Union to introduce a continental regulation system called European Train Control System (ETCS), which shall be used on high-speed tracks

* Corresponding author. Tel.: +39 051 20 9 3522; fax: +39 051 20 9 3527.
E-mail address: andrea.simone@unibo.it

10.1016/j.trpro.2020.03.030

because its components are specified for speeds up to 500 km/h. ETCS ensures full control of the train and it forces a safe reaction in case of irregularities. In most cases, this reaction is a controlled brake until the train has come to a stop. Data are transferred to the train by the Eurobalises system able to operate with passive transponder technology. The Eurobalises powering and the data reception are done by the onboard unit BTM and all the information are transferred to the trains after each passage over them (Kurz et al., 2007). Eurobalises transponders are installed on the railway sleepers and the loads applied by trains' air pressures could be destructive for the Eurobalise attack unite. As explained, these phenomena could represent a problem in terms of railway lines safety and management. A lack of communication between train and station operators can cause the unrevealed presence of a train in a railway section. For this reasons the study of the interaction between balise linkages systems and trains loads is necessary to avoid and prevent the unit detachments. When a train moves through air, it generates a slipstream that is defined as the airflow induced by a vehicle's movement. Generally, train slipstreams are characterized as highly - turbulent non-stationary regions of air, which to a static observer appears gradually-building gust punctuated with pulses of higher speed air. These air pulses are a result of gaps in the geometry of the vehicle and are generally much larger for freight trains than for passenger ones, therefore causing much larger pressure and velocity transients. Between 1972 and 2005 there were 26 reported slipstream-induced incidents on the UK rail network. These incidents included movement of trackside equipment, pushchairs and luggage (Flynn et al., 2014). In recent years, there has been considerable research that studies high-speed trains' aerodynamic performance. The basic tools used include full-scale tests, wind tunnel tests and computational fluid dynamics (CFD) (Xiao et al., 2013). In practice, it is measured at a fixed distance from the vertical center plane of the train. It is an important consideration for the aerodynamic performance but also for the operation of high-speed trains' infrastructures because of the significant pressure forces. The vortices move downwards and outwards beyond the passage of the train, causing the largest slipstream velocities to exist where people or infrastructure may be affected. The peak instantaneous slipstream velocities also occur in the near wake, however the magnitude and location of these peaks has been shown to be inconsistent in scaled moving-model experiments (Baker, 2010; Bell et al., 2014) and numerical investigations (Bell et al., 2017; Muld et al., 2012; Pii et al., 2014). Next to the study of slipstream phenomena, several studies have evaluated trains dynamic pressures effects on the bottom of the train with attention on movement effects on infrastructures and ballast. These studies have shown that the force required to initiate the stone movement is dependent on the grain size, shape and position in the track as well as the influence of the sleepers. Moreover has been shown that the aerodynamic load on the track increases with the roughness of the train and the train speed. From the studies of grains and high-speed video underneath trains and in wind tunnels is clear that, after the initiation of stone movement, they roll and bounce. Some stones may gain enough momentum to reach the train. Due to inertia, the acceleration of the stone is not instantaneous. Consequently, both peak loads and average loads are important. The probability of stone impact on the train increases with train length. It has been shown that ballast lowered below sleeper level reduces the susceptibility of the track whereas this is not an option with all track forms e.g. bi-block sleepers. It is also important to notice that the lateral and longitudinal resistance of the track are affected by the amount of ballast surrounding the sleepers. Moreover, the absence of ballast below the sleepers is introducing irregularities that can affect the stability of the train. The aim of this research was to assess the resistance of the balise support system, testing the stresses produced by the repeated passage of trains. Numerous tests have been done over the years to estimate the speed of the air flow under a train due to its motion at high speeds and, consequently, the force produced (Kim and Kim, 2007; Premoli et al., 2015; Rocchi et al., 2013). From these researches has been possible to understand the aerodynamic phenomena and associated forces that are generated under the train while in motion. From a first analysis, it was found that the causes that can generate this phenomenon are varied and sometimes difficult to study and analyze. Being able to identify the values of the forces that are generated on the ground below the train, provides values of reference to be used to verify the entire "Eurobalises" system.

2. Experimental Program

This analysis is aimed at studying the conditions that may lead to the separation of the balise from the railway sleepers. In particular, the connection between the "Balise" and sleeper is represented by a fixing steel H-plate. The Eurobalise is connected to the plate by means of four M10 bolts screwed into bushings, welded to the plate itself. Experimental laboratory tests were designed starting from the studies analyzed in the literature (Mazzotta et al., 2017, 2016; Rund et al., 2015). The tests aim to provide an analysis method capable of obtaining information about the

strength of the fixing system. The research was divided into two phases. In the first phase, laboratory tests were performed on the H-plate to find its limit resistance and elastic deformation due to the applied loads. In fact, considering the system and the dynamics of the damage generated by the train passage, it has been observed on site that the weakest element of the system is the H-plate, in particular the area of the welded connection between the bushings and the plate. To understand the phenomenon of detachment of the welded bushings and to evaluate their resistance, laboratory tests have been planned with three different load application types. Each test submits the only H-plate, without the balise-sleeper system, to a different action, applied directly to the bush. In fact, the welded bushings were subjected to pulled out, shear and bending to undergo stress similar to what is happening in the site. Since the three tests designed in different configurations, it was also necessary to design a different metal carpentry needed to adapt the system to the test machine. In the second phase, a laboratory test was conducted to analyze the behavior of the whole Eurobalise-cross system by simulating the aerodynamic load generated by the air on the upper surface of the system and subsequently comparing it with the test results from the first phase. Through these laboratory tests, it was possible to analyze the behavior of the welded connection for different types of load. In particular, the most significant values of strength and deformation were considered.

3. Mechanical assessment of the fastening system

In order to quantify the durability of the device, some tests were performed by subjecting the H-plate to three types of action without the balise-sleeper system. Tests were carried out with three types of loads: tensile (pull-out), shear and bending. In each test will be analyzed the static patterns used, and the test and the results obtained will be described.

1.1. 3.1 Tensile test (pull-out)

The pull-out test on the H-plate has the aim of evaluating the tensile force necessary to make the bushing detach from the steel H-plate. Being non-standardized tests, it was necessary to create a steelwork structure to adapt the system to the test machine. The metallic structure was made by fastening the H-bracket, bolting it down to a metal support with sufficient thickness to be considered rigid as shown in Figure 1a. Bolting the plate to the support, it has almost the same freedom of deformation that it has on site. The plate is bolted to a more rigid element by assimilating the behavior of the sleepers in the site, placing the bolting with the same configuration. The elements that make up the formwork of this test are the metal support, two screws (M10) and two nuts (M10) (Figure 1b, 1c). The task of the steel support is to simulate the sleeper that turns out to be much more rigid than the H-plate. For this test were used two different load speed equal to 5 daN/s (POP-A) and 30 daN/s (POP-B). No less than three tests were performed for each load configuration. In this way, it was possible to estimate quantitatively how the deformation of the H-plate affects the failure mechanisms. The stress was concentrated only on the welded area, resulting in the complete detachment of the bushing as occurred in the damaged elements on site. Observing the tests curves with the metal support in a single displacement-load chart (Figure 2), it is possible to note how the specimen assumes two different behaviors: a first elastic segment, up to a load of around 1000 N, followed by a second plastic section of the H-plate up until fail. All curves show that, on reaching the load of about 4 kN, there are small fluctuations meaning that the connection begins to give way. The displacement-time and load-displacement curves show an upward trend as time increases. The only visible difference regards the slope of the curves: in tests with slow load speed, curves grow less rapidly than the same with the fast load configuration. The values obtained from the "POP-A" and "POP-B" tests in the laboratory are shown in Figure 2. The average values of the maximum load obtained from three tests are therefore 5.02 kN for the POP-A test (velocity of 5 daN/s) and 6.23 kN for the POP-B test (velocity of 30 daN/s). The important result is represented by plastic deformation and strain induced in the component under the applied load around 1000 N. In the first part of the curves of Figure 2 is represented the trend in the elastic range of the specimen for the two load configurations. Figure 1d shows how a higher load velocity corresponds to a clear failure of the weld, also resulting in complete detachment of the bushing from the plate, as in the real case, and a higher value of maximum load. In conclusion, it was possible to assess the maximum tensile strengths of the welded connection. It was noted that, subject to traction, the plate undergoes significant deformation.

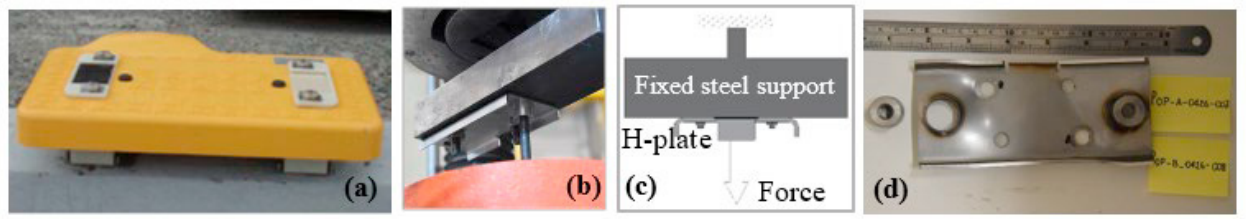

Fig. 1. Balise device fixed on a concrete railway sleeper (a). Design of the pull-out test (b). Static diagram (c). Failure after pull-out test (d).

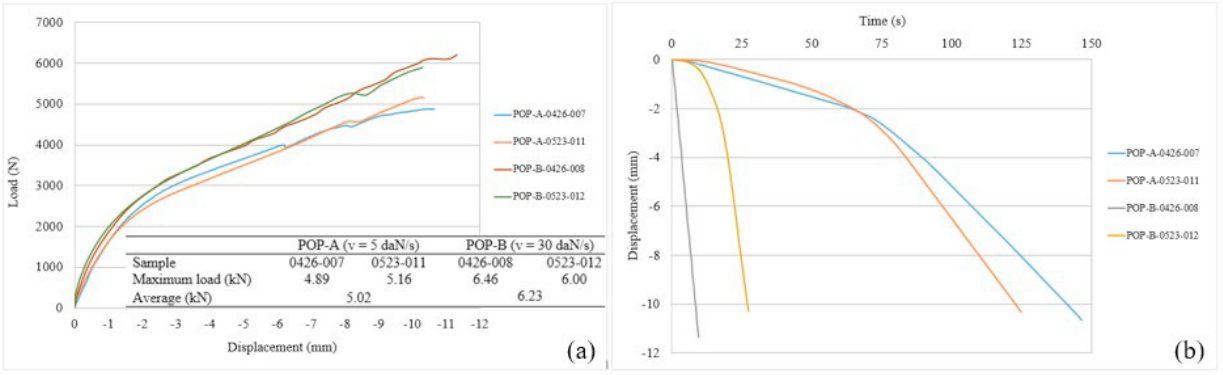

	POP-A (v = 5 daN/s)		POP-B (v = 30 daN/s)	
Sample	0426-007	0523-011	0426-008	0523-012
Maximum load (kN)	4.89	5.16	6.46	6.00
Average (kN)	5.02		6.23	

Fig. 2. POP-A and POP-B curves in load-displacement and displacement-time. In the table the maximum load values at breaking point.

1.2. 3.2. Shear Test

The shear test on the H-plate has the aim of evaluating the tensile force necessary to make the bushing detach from the steel H-plate. In order to apply a shearing action on the bushing, a static layout was devised, as shown in Figure 3.

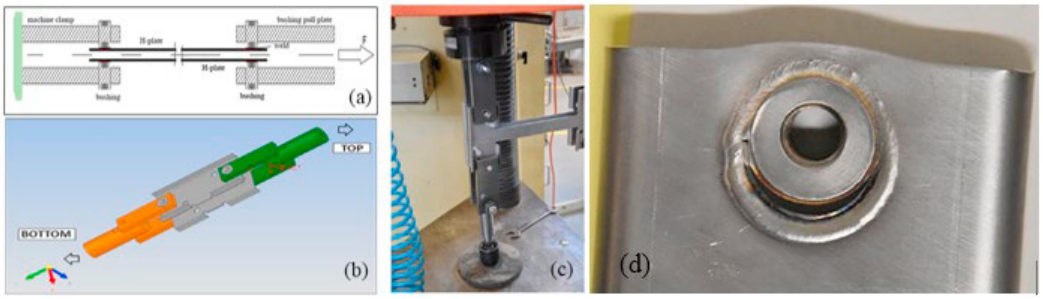

Fig. 3. Shear test static diagram (a). 3D Static layout for shear test (b). Installation details (c). Failure detail (d).

The test was performed by maintaining an advancement speed of 10 daN/s. The failure obtained was characterized by the bushing hole becoming oval, qualitatively similar to the results found on site. No less than three tests were performed for each load configuration. Figure 4 shows the charts corresponding to the three samples for the bound shear test (PTV), to assess how actions and displacements vary with time.

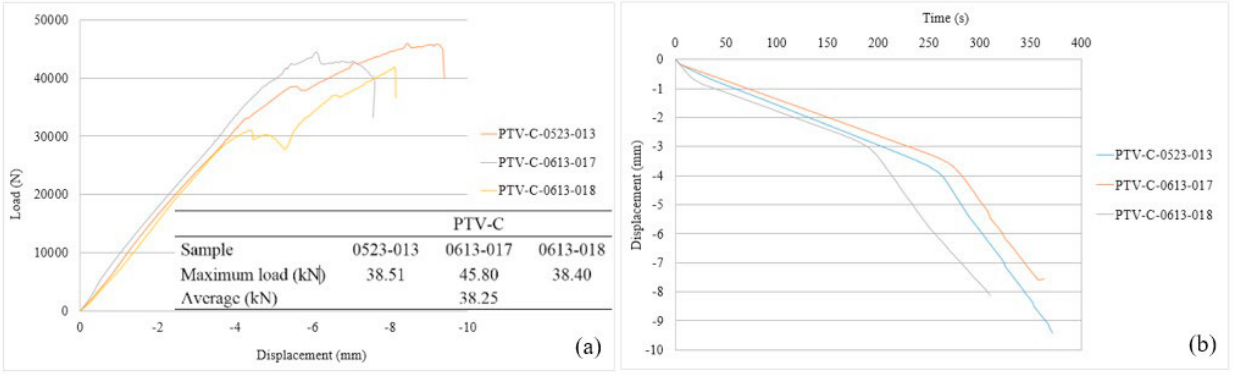

Fig. 4. PTV-C displacement vs time (a) load vs time (b). In the table the maximum load values at breaking point.

It is possible to observe that three samples, at a time of about 200 seconds and a load of about 25 kN (equal to displacements of about 3 mm), present a variation in the slope of the curves. They assume a linear elastic behavior of the system up to the value of load equal to 25 kN and subsequently the plastic phase, at the end of which the system breaks. In particular, the rupture primarily affects the weld, as it does not have an effective detachment of the bushing from the H-bracket. The table in Figure 4 shows the loads at the breaking point of the various PTV tests. The average of the maximum load reached by the PTV-C test is equal to 38.25 kN, corresponding to the shear strength of the bushing weld with a load speed equal to 10 daN/s. The result of greatest importance is represented by the plastic deformation and strain induced in the component under the applied load around 1000 N. In the first part of the curves of Figure 4(a) is represented the trend in the elastic range of the specimens for the load configuration. Figure 3(d) shows the failure detail at the end of the test.

3.3. Bending test

This test, carried out to analyze the attachment of the balise to the sleeper, is a shear and moment test, whose objective is to assess the system resistance to failure mechanisms due to bending. For this test, the specimen was made coupling two H-plates and screwing in four bolts, one per bushing (Figure 5d).

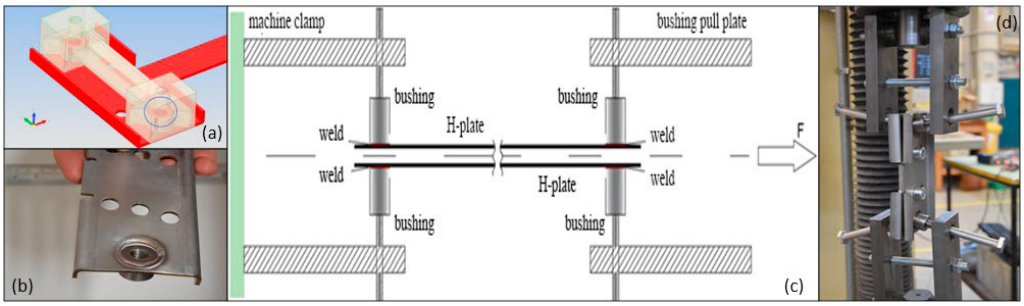

Fig. 5. Detail of nylon element belonging to the BBS system (a). Breakage achieved during bending test (b). Bending test-mounting system (c). Bending test static diagram (d).

The structure used is the same as the one used for the shear test with the addition of four spacers placed between the laminated steel plate brackets and the machine fastening system. The spacers are necessary to keep the steel plates on an axis with the point of application of force. The beam applying the force, measuring 15 mm, represents the point of contact between the nylon elements and the bushing. Figure 5a shows two 3D images that clarify the point of contact referred to. Figure 5a represents the nylon element having two cylindrical holes 15 mm deep, adapted to accommodate the bushings. It is possible to see the coupling of the two elements and the point of contact between the

support surfaces highlighted in the blue circle. Figure 6 shows results referred to the three bending test performed. The trends presents a plastic phase up to a load of approximately 1000 N. Analyzing the load-displacement diagram of the bending test, it is found that the curves show a similar linear and plastic elastic behavior. The table in Figure 6 lists the loads at fail of the different bending tests. The average of the maximum load values reached by the PMV15-C test is equal to 7.56 kN. This value corresponds to the bending resistance of the bushing weld as a function of load velocity equal to 10 daN/s. The result of greatest importance is represented by the yield strength that occurs around 1000 N. The first part of the curves in Figure 6 shows the trend in the elastic range of the specimen for load configurations. It is important to highlight the difference between the orders of magnitude of the breaking loads of the PTV and PMV tests, in which we have respectively the following average values of fail of 38.25 kN and 7.56 kN.

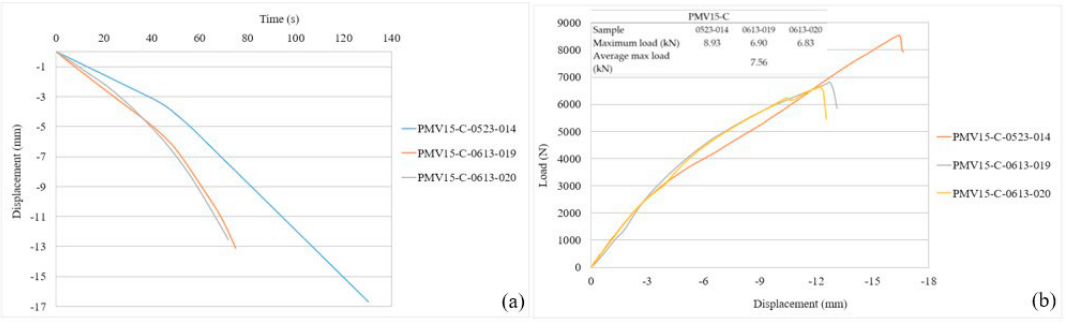

Fig. 6. PMV displacement-time (a) and load-displacement (b). In the table the maximum load values at breaking point.

This difference makes it possible to exclude the existence of just the shearing action on the BBS system, the average breaking load for shear being too high a value to achieve with only the aerodynamic action generated by the passage of a high-speed train without there being contact between the two.

4. Full-scale tests for the mechanical assessment of the balise-sleeper fastening

In this paragraph it will be described the test designed and realized on the entire Eurobalise fastening system in regular operating configuration. Attention was primarily focused on the S16 sleeper, monoblock concrete without armature in the central part. The balise is connected to the sleeper by means of the BBS fastening support bolted in a symmetrical manner. Test machine chosen is a common tensile/compression one (Figure 7a, 7b, 7c).

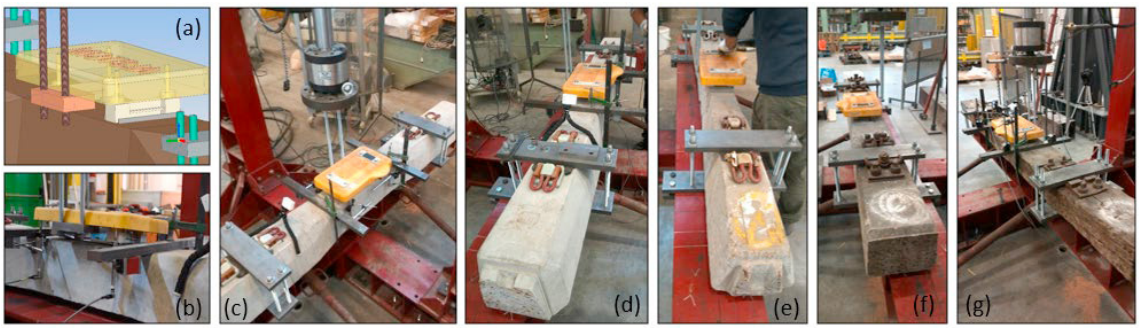

Fig. 7. The restraining system (a). Test Execution (b). Structure for applying load to the system (c). Type of sleepers: S16 (d), S89 (e), SP90 (f) and Wood (g).

A steel structure was designed to bind the sleeper to the steel beam. The size of the plates and screws were the result of evaluations of compatibility with the machinery structure chosen for the test, the types of sleepers to be tested and from the configuration of the load to be applied. In particular, the test system has been designed to avoid deformation and movement. The restraining system consists of two steel supports, two screws, two nuts and two washers (M16 class 8.8). The function of this support is to connect the piston load head and the balise. It was decided to set the machine using the average speed of about 10 daN/s, in order to more easily control the deformation and prevent damage or unintended consequences. In order to record the system displacements, four LVDT transducers were installed to detect the movement of the balise in the four vertices. Depending on the type of sleeper and the system to be tested, transducers of different sizes were installed in relation to the deformation expected. Starting from values recorded by the system, results have been analyzed by highlighting the maximum load reached.

4.1. Comparison of the results obtained from the different sleepers.

Tests on four types of sleepers were performed (Figure 7d, 7e, 7f, 7g). In particular, for all performed tests comparisons were made about the system's load-displacement diagrams (Figure 8a), the load-time diagrams (Figure 8b). In Table 1 are listed the load values at failure and the displacement value of the edge of the boa during the loading phase.

The curves show the first elastic segment in which there is a direct proportionality between load and displacement. Subsequently, the curves change slope and there is a first plasticization of the H-plate at the connection with bushing, similar to the results obtained in the other tests described. The first parts of the curves tend to almost overlap, while in the second phase they tend to move away as weld failure mechanisms becomes imminent.

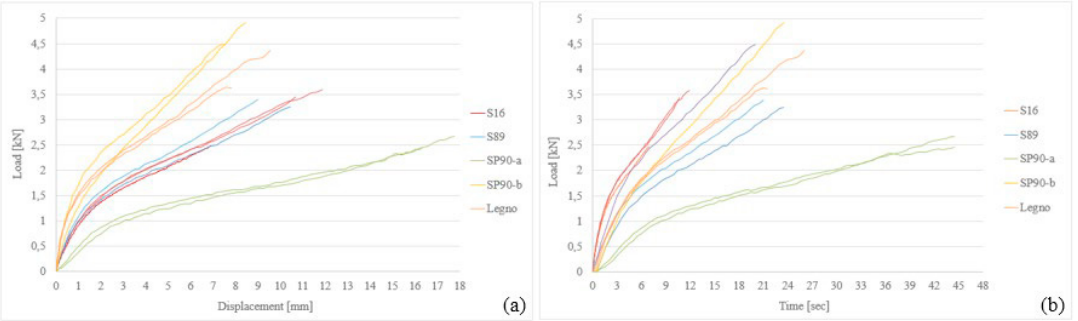

Fig. 8. Load-displacement (a) and load-time curve (b) of tested sleepers.

Table 1. Results of the full scale test (a - unbolted side; b - bolted side).

				Average values		Max values	
		Load [kN]	**Displ [mm]**	**Load [kN]**	**Displ. [mm]**	**Load [kN]**	**Displ. [mm]**
S16	**PG01**	2.40	5.49	3.0	9.6	3.4	12.7
	PG02	3.10	12.74				
	PG03	3.44	10.68				
S89	**PG04**	3.25	9.02	3.3	9.7	3.4	10.4
	PG05	3.40	10.44				
SP90	**PG06-a**	2.67	17.75	2.6	17.1	2.7	17.7
	PG07-a	2.45	16.37				
	PG08-b	4.49	7.47	4.7	8.0	4.9	8.5
	PG09-b	4.91	8.47				
WOOD	**PG10**	4.36	9.56	4.0	8.7	4.4	9.6
	PG11	3.62	7.79				

Starting with the different types of sleepers, the resistance of the system varies based on the fastening system used between the plate and the sleeper. In the welded area, there is a localized concentration of stresses due to a dual action of traction and bending moment that are generated on the system. Figure 8a reports the load-displacement performance of the systems tested, where the elastic limit comes after a displacement of about 3 mm corresponding to a load of approximately 1.5 kN. With regard to the trend of the load vs time (Figure 8b), it was noted that the elastic limit occurs after about 3 seconds with a load of approximately 1.5 kN. Overall the curves show a similar trend, therefore the values obtained can be considered typical for this type of configuration to the exclusion of the tested type of system installed on the SP90-a sleeper as it utilizes a different fastening system.

4.2. Interpretation of the test results.

Following the laboratory tests, the element of the Eurobalise-sleeper system that always is damaged is the fixing plate, in particular the welded connection between the plate and the bushing. The objective of the study is to estimate, starting from the damaged element, the resistance of the system under the load action, and specifically the resistance of the welded connection between the bushing and the H-plate. Based on 3D system drawings to better illustrate the system, a 2D reference diagram has been developed as shown in Figure 9a. This simplification has made it possible to realize simple and fast structural analysis and to obtain reference values. The dimensions of the static diagram are dictated by the geometry of the elements identified as parts of the system that interact during the test (Figure 9a). The elements considered for the construction of the frame are the balise, the M10 bolts, the bushing and the portion of the plate that extends from the fastening screw on the outermost end of the plate. In particular, the axis was considered of the upper side of the balise, the bolt, the bushing and the plate. The maximum load obtained was then applied to the extremity of the frame so as to reproduce the same configuration of the laboratory test as shown in Figure 9b. Under the action of the load applied by the machine, the system is deformed. The impossibility of displacement of the entire system due to the mounting on the sleeper and the distribution of the rigidity of the elements, that make up the system itself, counteracts the displacement of the bushing, so the welded connection reaches the ultimate breaking point and becomes damaged (Figure 9e).

The phenomenon generated has been interpreted as a lever system. If resistance (or load) is in the middle, the effort is applied on one side of the resistance and the fulcrum is located on the other side. The layout considered as rigid element the balise which represents the lever, the core is placed at the point of the balise-bushing fastening with M10 bolt, while the resistance is interposed between the point of application of the load and the fulcrum (Figure 9c).

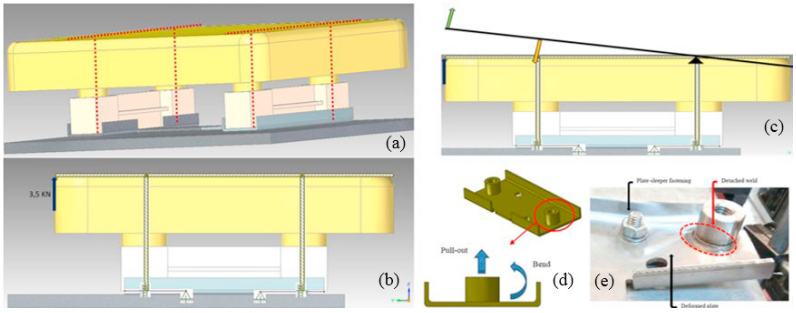

Fig. 9. Static diagrams of the system (a). Load application to the static diagram (b). Lever behavior (c). Stress calculated on the bushing (d). Detachment of the weld and plate deformation (e).

Alternatively, structural reactions have been calculated with the software Ftool (Figure 10b). Having defined all the elements necessary for the simulation, the resolution provides the deformed configuration and the magnitude of stress and displacement in correspondence with the welded connection between the bushing and the plate. The results obtained are of the same order of magnitude as those obtained by resolution with the lever mechanism: the traction

value is equal to -4.87 kN (representative of the pull-out force on the bushing), the value of the bending stress is equal to 0.23 kNm (representative of the bending moment generated on the welded connection between the plate and bushing Mb). The objective is to compare the two combined stresses of traction and bending moment that are generated during the full scale test on the welded connection between the bushing and the plate. These actions have been identified, quantified and correlated to the corresponding values of the tests on the steel H-plate. In fact, the comparison shows that the pull-out values and the bending moment values are comparable (Table 2). The correlation found allowed to extend the investigation field. In particular, taking into account the studies conducted by Wei et al., (2011), the potential pressure values acting on the surface of the Eurobalise have been extrapolated and, note the surface (22.5 x 44.5 cm^2), three potential forces and the generated moment acting on the system have been identified for various train speed (Table 3).

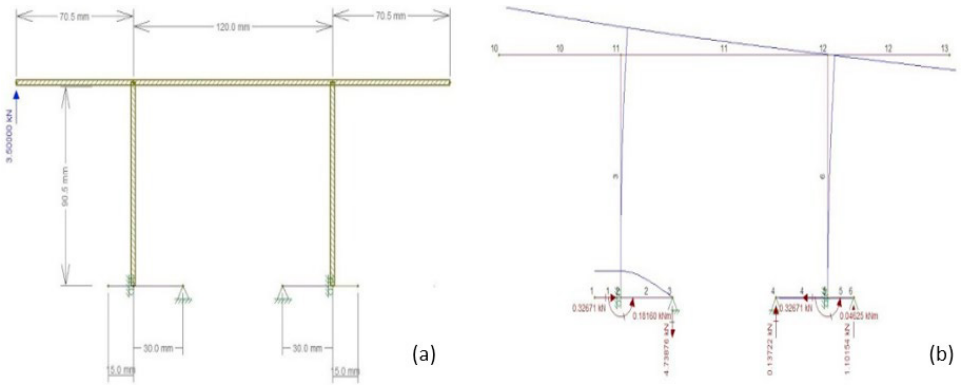

Fig. 10. Implementation of the diagram in the Ftool program (a). Resolution and deformed in Ftool (b).

Table 2. Comparison of test results on pull-out force and bending moment.

Test	Pull-Out force [kN]	Moment values [kNm]
Steel H-plate	6	0.12
Full scale	5	0.19

Table 3. Pressure Transient Values for Various Train Speed.

Speed [km/h]	Pressure [Pa]	Pull-Out Force [kN]	Moment Values [kNm]
200	600	0.085	0.003
250	1000	0.15	0.005
300	1500	0.23	0.008

These values can be useful as a parameter to evaluate the actions on the balise. From Table 3, comparing a "project" dynamic action acting on the ground below a passing train with the quasi-static "resistant" action, founded through the experimental test, it is possible to determine that exist a different order of magnitude between the two actions. Even considering different load times, it makes possible to guarantee a degree of confidence amply sufficient to account for aerodynamic actions and confirms the reliability of the connection of the balise to the sleepers even for the passage of high-speed trains. As confirmation, a dynamic test was performed consisting of 4 steps with 10,000 load-unload cycles each with a frequency equal to 10 Hz, a load velocity of 0.012 mm/s and a load applied ranging between 100-200 N (average value increased by 50% compared to the "project" dynamic action). The test is done with displacement control and the instrumentation is the same as the sleeper test with static load. The 10,000 cycles are derived from the starting assumption that on average a train passes over a given spot about 130 times, for an annual total that exceeds 40,000. Comparing displacements at the end of each step with the initial configuration of the plate, we found that the balise has no residual deformation, confirming the locked position of the plate.

5. Conclusions

The causes that can generate the "Eurobalise" detachment from the sleepers are several and sometimes difficult to study and analyze. The purpose of this paper was to identify the resistance of the Eurobalise fastening system on different types of sleepers, in particular the actions that contribute to the damage of the balise-sleeper connection after the passage of the train. Starting from the in-depth analysis of the various aerodynamic studies present in the literature, the applied force on the balises has been obtained and from tests carried out on the H-plate it has been found that the weld breaks at the base of the connection between the bushing and the plate, the point where the most stress is focused. From tests carried out on the sleeper it was found that the resistance of the system is practically the same for all types of sleepers (wood and concrete) and not depend on the system used to fasten the plate to the sleeper. The only case in which the resistance varies is the SP90 sleeper, which uses a different fastening system with different kind of restraint. Resistance to fail of the bushing-plate connection subjected to different stress actions and resistance to breakage of the balise-sleeper system have been identified and can be used as a reference during the installation phase.

6. References

Baker, C., 2010. The flow around high speed trains. Journal of Wind Engineering and Industrial Aerodynamics 98, 277–298. https://doi.org/10.1016/j.jweia.2009.11.002

Bell, J.R., Burton, D., Thompson, M., Herbst, A., Sheridan, J., 2014. Wind tunnel analysis of the slipstream and wake of a high-speed train. Journal of Wind Engineering and Industrial Aerodynamics. https://doi.org/10.1016/j.jweia.2014.09.004

Bell, J.R., Burton, D., Thompson, M.C., Herbst, A.H., Sheridan, J., 2017. A wind-tunnel methodology for assessing the slipstream of high-speed trains. Journal of Wind Engineering and Industrial Aerodynamics 166, 1–19. https://doi.org/10.1016/j.jweia.2017.03.012

Flynn, D., Hemida, H., Soper, D., Baker, C., 2014. Detached-eddy simulation of the slipstream of an operational freight train. Journal of Wind Engineering and Industrial Aerodynamics. https://doi.org/10.1016/j.jweia.2014.06.016

Kim, J.Y., Kim, K.Y., 2007. Experimental and numerical analyses of train-induced unsteady tunnel flow in subway. Tunnelling and Underground Space Technology 22, 166–172. https://doi.org/10.1016/j.tust.2006.06.001

Kurz, T., Harnstein, R., Schweinzer, H., Balik, M., Mayer, M., 2007. Time synchronization in the eurobalise subsystem, in: 2007 IEEE International Symposium on Precision Clock Synchronization for Measurement, Control and Communication, ISPCS 2007 Proceedings. https://doi.org/10.1109/ISPCS.2007.4383776

Mazzotta, F., Lantieri, C., Vignali, V., Simone, A., Dondi, G., Sangiorgi, C., 2017. Performance evaluation of recycled rubber waterproofing bituminous membranes for concrete bridge decks and other surfaces. Construction and Building Materials. https://doi.org/10.1016/j.conbuildmat.2017.01.058

Mazzotta, F., Simone, A., Vignali, V., Lantieri, C., Sangiorgi, C., Dondi, G., 2016. Pull-out tests on bituminous specimens with steel wire mesh reinforcements, in: Functional Pavement Design - Proceedings of the 4th Chinese-European Workshop on Functional Pavement Design, CEW 2016. https://doi.org/10.1201/9781315643274-98

Muld, T.W., Efraimsson, G., Henningson, D.S., 2012. Flow structures around a high-speed train extracted using Proper Orthogonal Decomposition and Dynamic Mode Decomposition. Computers and Fluids. https://doi.org/10.1016/j.compfluid.2011.12.012

Pii, L., Vanoli, E., Polidoro, F., Gautier, S., Tabbal, A., 2014. A full scale simulation of a high speed train for slipstream prediction.

Premoli, A., Rocchi, D., Schito, P., Somaschini, C., Tomasini, G., 2015. Ballast flight under high-speed trains: Wind tunnel full-scale experimental tests. Journal of Wind Engineering and Industrial Aerodynamics. https://doi.org/10.1016/j.jweia.2015.03.015

Rocchi, D., Schito, P., Tomasini, G., Giappino, S., Premoli, A., 2013. Numerical-experimental study on flying ballast caused by high-speed trains, in: 6th European and African Conference on Wind Engineering, EACWE 2013.

Rund, M., Procházka, R., Konopík, P., Džugan, J., Folgar, H., 2015. Investigation of Sample-size Influence on Tensile Test Results at Different Strain Rates, in: Procedia Engineering. pp. 410–415. https://doi.org/10.1016/j.proeng.2015.08.086

Wei, Y., Li, H., Wang, L., 2011. Simulation analysis and validation on aerodynamics of tunnels on high speed railways. Proceedings of 2011 International Conference on Electronic and Mechanical Engineering and Information Technology, EMEIT 2011 2, 972–975. https://doi.org/10.1109/EMEIT.2011.6023257

Xiao, J., Huang, Z., Chen, L., 2013. Review of aerodynamic investigations for High Speed train. Mechanics in Engineering 35, 1–12. https://doi.org/10.6052/1000-0879-13-063